Endurance degradation mechanisms in TiN\Ta_2O_5\Ta resistive random-access memory cells

C. Y. Chen,[1,2,a)] L. Goux,[1] A. Fantini,[1] S. Clima,[1] R. Degraeve,[1] A. Redolfi,[1] Y. Y. Chen,[1] G. Groeseneken,[1,2] and M. Jurczak[1]
[1]*imec, Kapeldreef 75, B-3001 Leuven, Belgium*
[2]*KU Leuven, Dept. Elektrotechniek ESAT-MICAS, B-3001 Leuven, Belgium*

(Received 2 December 2014; accepted 24 January 2015; published online 2 February 2015)

Impact of set/reset pulse duration and amplitude on the endurance failure modes of TiN\Ta_2O_5\Ta cells is investigated and is related to interaction between Oxygen and TiN bottom electrode during reset. Hourglass electrical switching simulation of conductive filament temperature during reset transient and *ab-initio* calculation of reaction energy further support this degradation mechanism. Based on this understanding, endurance improvement is achieved by using shorter reset pulse and/or using inert Ru bottom electrode. © *2015 AIP Publishing LLC*.
[http://dx.doi.org/10.1063/1.4907573]

Recent progress in transition metal oxides (TMO) based resistive-switching random-access memory (RRAM) research has drawn attention from high-performance application due to its improvement in reliability, especially in the write endurance achievements for both HfO_2[1–3] and Ta_2O_5[4–6] based devices. Although failure modes are analyzed in these works[1–7] and alleviated by programming methodology,[8] there is still no clear understanding of the physical mechanisms causing endurance degradation. In this letter, we systematically study the impacts of pulse-programming parameters on endurance characteristics of scaled TiN\Ta_2O_5\Ta devices. By means of hourglass (HG) electrical switching simulation and *ab-initio* calculation, we analyze the physics leading to switching failure and draw some guidelines toward improvements.

RRAM crossbar devices were integrated onto select transistor in a 1-Transistor\1-Resistor (1T1R) circuit scheme [Figs. 1(a) and 1(b)]. Amorphous atomic-layer-deposition (ALD) Ta_2O_5 layers (6 nm) deposited at 250 °C using $TaCl_5$ as precursor and H_2O as oxidant were sandwiched between stoichiometric TiN (30 nm) bottom electrode (BE) and Ta (10 nm) top electrode (TE) realized by physical-vapor-deposition (PVD) [Fig. 1(c)]. Chemical composition of Ta_2O_5 layer was confirmed in previous work.[6] Device size is 100 nm $\times$ 100 nm. The switching current I_{cc} is fixed at 50 μA, as modulated by the word-line (WL) voltage during forming and set. Positive (respectively, negative) voltage is applied to the bit-line (BL) for set (respectively, reset) programming. DC forming and switching characteristics are shown in Fig. 1(d). AC-pulse experiments were carried out using square pulses having edges fixed to 3 ns and a top-plateau duration defining the pulse-width (PW). Devices are effectively set/reset using pulse amplitudes V_{set} and V_{reset} lower than 1.5 V and PW $\leq$ 10 ns.[6] In all endurance tests, a statistical sample of more than 20 devices is used.

Fig. 2(a) shows endurance characteristics obtained in standard test conditions ($PW_{set} = PW_{reset} = 10$ ns, $V_{set} = 2.5$ V, and $V_{reset} = -1.5$ V). The current read-out of Low/High Resistance State (LRS/HRS) is measured by a DC source meter at 0.1 V. While the standard test condition results in a lifetime of $\sim 10^6$ switching cycles, failing to reset (failure mode A), the increase of V_{reset} to -1.75 V results in a failure to set (mode B) [Fig. 2(b)]. Interestingly, very similar endurance characteristics and failure mode B is obtained for increased PW_{reset} [Fig. 2(c)]. In all cases, HRS fluctuates more than LRS due to lower number of oxygen-vacancy particles (n_c) in the filament constriction.[9] With longer PW_{reset} [Fig. 2(c)], this dispersion can be better controlled.

To further investigate these failure modes, HG simulations of conductive filament (CF) temperature during reset were performed for two different reset amplitudes. Note the temperature is estimated from the power divided by n_c in the CF constriction, as described in Refs. 9 and 10. For $V_{reset} = -1.5$ V, although decreasing rapidly in the first tens of ns, the CF temperature remains at >500 K and fluctuates considerably during the entire reset pulse duration [Fig. 3(a)]. This high temperature is due to the large residual current density though the reset-induced narrower quantum-point-contact (QPC) constriction cross-section, while the temperature fluctuations are a signature of the thermal-induced competition between formation of stable and mobile

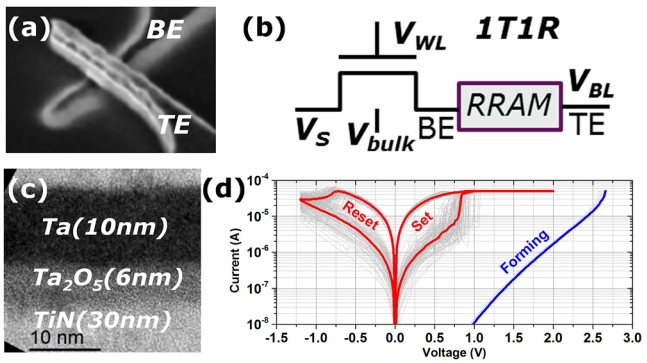

FIG. 1. (a) Top-view SEM image of the RRAM cross-bar cell and (b) schematics of the 1T1R memory cell integration. (c) Cross-section TEM image of the TiN\Ta_2O_5\Ta device and (d) DC forming and switching characteristics of several devices, where gray lines are traces of different devices, and red and blue lines are median traces.

a)Electronic mail: michael.chen@imec.be

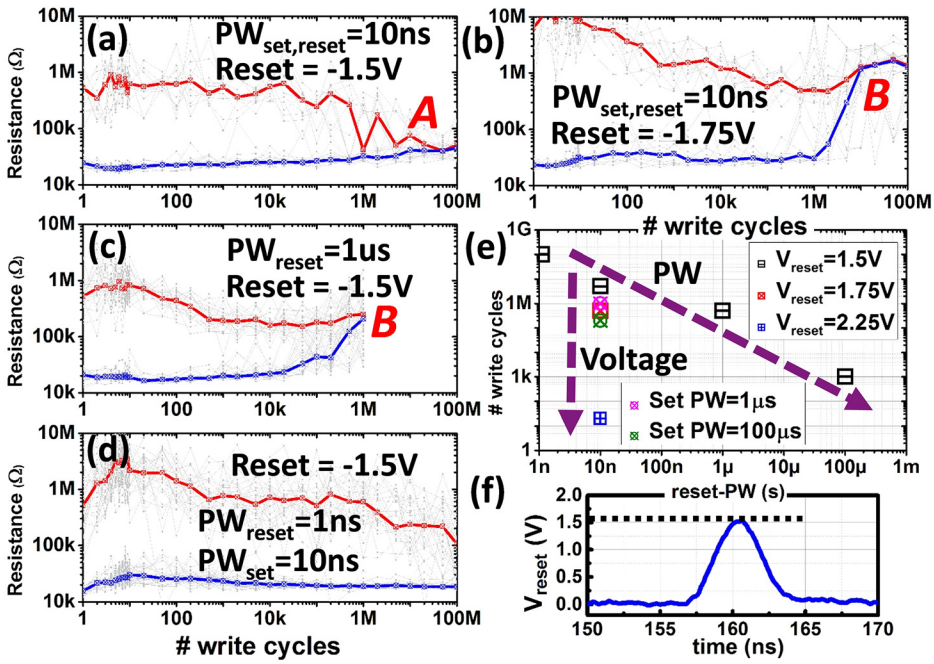

FIG. 2. AC endurance characteristics measured (a) under standard condition, (b) for increased $V_{reset} = -1.75$ V, (c) for increased $PW_{reset} = 1$ μs, and (d) for decreased $PW_{reset} = 1$ ns; blue and red lines are LRS/HRS median traces. (e) Overview results of endurance lifetime depending on V_{reset}, PW_{reset}, and PW_{set}. (f) Snapshot oscilloscope trace obtained for $PW_{reset} = 1$ns.

V_o reaching a state of dynamic balance.[9] Due to direct impact on power, increasing V_{reset} to -1.75 V leads not only to a much higher CF temperature but also to larger fluctuation amplitudes [Fig. 3(a)].

On the other hand, varying PW_{set} and V_{set} from the standard test conditions did not result in strong impact on endurance lifetime [Fig. 2(e)]. Consistently, the CF temperature estimated from HG simulations during set pulse remained limited and more stable over the entire pulse duration [Fig. 3(b)], which is related to larger n_c after set transient. The absence of V_{set} effect is due to the snapback of the voltage dropping on the cell to the transition voltage $V_{trans} \sim 0.5$ V, limiting the stand-by power during set.[10]

Based on these results, using shorter PW_{reset} and moderate V_{reset} appears most effective in improving endurance. Fig. 2(d) shows the increase of endurance lifetime to $\sim 10^8$ cycles obtained using shortest possible reset pulse allowed by the pulse-generator instrument (HP8110) [Fig. 2(f)]. A summary of endurance lifetime as a function of different test conditions is shown in Fig. 2(e).

From earlier works, we know that the CF constriction is located close to the BE interface.[11] We thus calculated by *ab-initio* the free enthalpy of oxydation ΔG of BE materials by Oxygen (O) from the CF. Large $\Delta G \sim 6$ eV is obtained for ideal TiN crystal, however it drops to -2 eV for pure Ti [Fig. 4(a)]. In PVD-deposited TiN layers, any point defects such as Nitrogen vacancies (V_N) or Ti dangling bonds will have the same effect of locally decreasing ΔG and result in TiN oxidation, which is also in agreement with previous calculations of Bradley *et al.*[12] Hence, gradual TiN oxidation by these microscopic mechanisms is likely induced by the large reset field and temperature during endurance, leading finally to failure to set (B) due to difficult O-detrapping from TiN.[13] On the other hand, endurance with lower reset field and temperature may be insufficient for TiN oxydation, however sufficient for O in-diffusion, as interstitials[13] or simply through defects like grain boundaries, which would lead finally to failure to reset (A). Figs. 4(c) and 4(d) show schematic descriptions of failures.

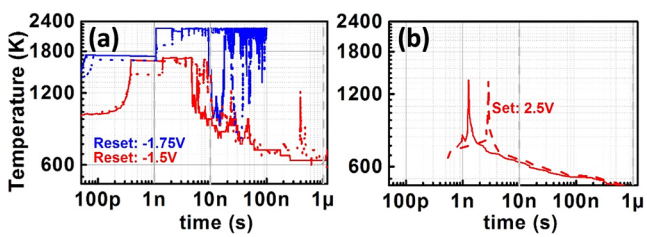

FIG. 3. (a) Profiles of the CF temperature obtained during reset pulses for $V_{reset} = -1.5$ V (red) and $V_{reset} = -1.75$ V (blue) and (b) during set pulses, as obtained from hourglass simulation; each condition contains 2 simulations (solid and dash lines). Temperature fluctuations are observed during the entire reset pulse duration and are significantly increased with higher amplitude.

From *ab-initio*, the use of Ru BE results not only in restored large ΔG but also in reduced O in-diffusion [Fig. 4(b)], which should improve the immunity to failures B and A, respectively [Fig. 4(e)]. The crystal structure used in calculation for Ru is hexagonal closed packed and cubic for TiN. We also performed *ab-initio* calculation for rutile RuO_2 and the lowest diffusion E_a obtained was ~ 1.5 eV, similarly to Ru BE, which means RuO_2 would theoretically behave as O-barrier and might as well be an option allowing increased endurance lifetime.

Experimental endurance tests on Ru\$Ta_2O_5$\Ta devices confirmed the *ab-initio* predictions, as shown in Fig. 4(f). Even for large temperatures and fields associated to the large reset pulse $V_{reset} = -2$ V tested with $PW_{set} = PW_{reset} = 10$ ns, no failure was observed before 10^7 write endurance cycles. HRS fluctuation remains similar to Fig. 2(a) suggesting that the bottom electrode material does not affect n_c but mainly impacts the endurance lifetime.

To conclude, in this letter, we investigate the endurance degradation mechanisms of TiN\Ta_2O_5\Ta RRAM cells. We show that it is strongly correlated to Oxygen interaction with TiN bottom electrode material during reset pulse-programming. By limiting the interaction with short reset

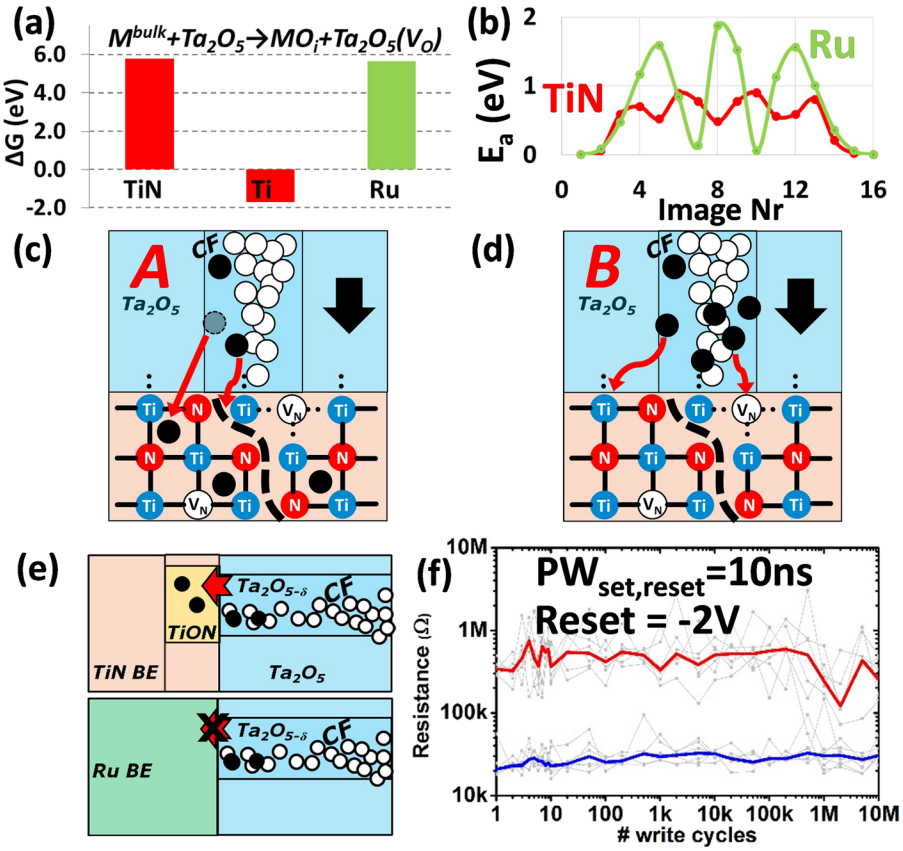

FIG. 4. *Ab-initio* calculation of the energy barrier required for O (a) to react (ΔG) with BE materials and (b) to diffuse (E_a) in TiN and Ru; (c) and (d) schematics describing possible degradation mechanisms accounting for failure modes A and B, where O is shown in black. (e) Schematics depicting suppressed O-induced BE degradation during switching using Ru. (f) Endurance characteristics obtained on Ru\Ta_2O_5\Ta devices tested in standard condition except for $V_{reset} = -2$ V.

pulse width and moderate amplitude, endurance lifetime may be extended to 10^8 cycles. Ru BE material was also used to confirm the endurance degradation analysis.

The authors acknowledge the partial funding by imec's Industrial Affiliation program on RRAM.

[1]H. Y. Lee, Y. S. Chen, P. S. Chen, P. Y. Gu, Y. Y. Hsu, S. M. Wang, W. H. Liu, C. H. Tsai, S. S. Sheu, P. C. Chiang, W. P. Lin, C. H. Lin, W. S. Chen, F. T. Chen, C. H. Lien, and M.-J. Tsai, IEEE Int. Electron Devices Meet. **2010**, 19.7.1–19.7.4.
[2]A. Fantini, L. Goux, A. Redolfi, R. Degraeve, G. Kar, Y. Y. Chen, and M. Jurczak, Symp. VLSI Technol. **2014**, 242–243.
[3]Y. Y. Chen, B. Govoreanu, L. Goux, R. Degraeve, A. Fantini, G. S. Kar, D. J. Wouters, G. Groeseneken, J. A. Kittl, M. Jurczak, and L. Altimime, IEEE Trans. Electron Devices **59**(12), 3243–3249 (2012).
[4]J. J. Yang, M.-X. Zhang, J. P. Strachan, F. Miao, M. D. Pickett, R. D. Kelley, G. Medeiros-Ribeiro, and R. S. Williams, Appl. Phys. Lett. **97**(23), 232102 (2010).
[5]M. J. Lee, C. B. Lee, D. Lee, S. R. Lee, M. Chang, J. H. Hur, Y. B. Kim, C.-J. Kim, D. H. Seo, S. Seo, U.-I. Chung, I.-K. Yoo, and K. Kim, Nat. Mater. **10**, 625–630 (2011).
[6]L. Goux, A. Fantini, A. Redolfi, C. Y. Chen, F. F. Shi, R. Degraeve, Y. Y. Chen, T. Witters, G. Groeseneken, and M. Jurczak, Symp. VLSI Technol. **2014**, 162–163.
[7]B. Chen, Y. Lu, B. Gao, Y. H. Fu, F. F. Zhang, P. Huang, Y. S. Chen, L. F. Liu, X. Y. Liu, J. F. Kang, Y. Y. Wang, Z. Fang, H. Y. Yu, X. Li, X. P. Wang, N. Singh, G. Q. Lo, and D. L. Kwong, IEEE Int. Electron Devices Meet. **2011**, 12.3.1–12.3.4.
[8]J. Song, D. Jee, J. Woo, Y. Koo, E. Cha, S. Lee, J. Park, K. Moon, S. H. Misha, A. Prakash, and H. Hwang, IEEE Electron Device Lett. **35**(6), 636–638 (2014).
[9]R. Degraeve, A. Fantini, N. Reghavan, Y. Y. Chen, L. Goux, S. Clima, S. Cosemans, B. Govoreanu, D. J. Wouters, Ph. Roussel, G. S. Kar, G. Groeseneken, and M. Jurczak, Symp. VLSI Technol. **2013**, 98–99.
[10]R. Degraeve, A. Fantini, S. Clima, B. Govoreanu, L. Goux, Y. Y. Chen, D. J. Wouters, Ph. Roussel, G. S. Kar, G. Pourtois, S. Cosemans, J. A. Kittl, G. Groeseneken, M. Jurczak, and L. Altimime, Symp. VLSI Technol. **2012**, 75–76.
[11]L. Goux, A. Fantini, G. S. Kar, Y. Y. Chen, N. Jossart, R. Degraeve, S. Clima, B. Govoreanu, G. Lorenzo, G. Pourtois, D. J. Wouters, J. A. Kittl, L. Altimime, and M. Jurczak, Symp. VLSI Technol. **2012**, 159–160.
[12]S. R. Bradley, K. P. McKenna, and A. L. Shluger, Microelectron. Eng. **109**, 346–350 (2013).
[13]R. K. Pandey, R. Sathiyanarayanan, U. Kwon, V. Narayanan, and K. V. R. M. Murali, J. Appl. Phys. **114**, 034505 (2013).